Non-Contact Measurements of Water Jet Spreading Width with a Laser Instrument

Yuki Funami, Ryo Hasuya, Kotaro Tanabe and Yuji Nakanishi

Kanagawa University: 3-27-1, Rokkakubashi, Kanagawa-ku, Yokohama, Kanagawa, 221-8686, Japan

Jet spreading width is one of the important characteristics of water jets discharging into the air. Many researchers have dealt with measuring this width, and contact measuring methods on the water jet surface were employed in a lot of the cases. In order to avoid undesirable effects caused by the contact on the jet surface, we introduce non-contact measuring methods with a laser instrument to the measurements of jet spreading width. In measurements, a transmitter emits sheet-like laser beam to a receiver. The water jet between the transmitter and the receiver interrupts the laser beam and makes a shadow. The minimum and maximum values of the shadow width are measured. In addition, pictures of the water jet are taken with a scale, and the shadow width is measured from the pictures. The experiments on various needle strokes were performed. Three kinds of width consistent with the jet structure were obtained. In the results, it can be concluded that our non-contact measuring methods are feasible. The data of jet spreading widths and jet taper were obtained and are useful for future applications.

Keywords: Water jet, Jet spreading width, Jet taper, Non-contact measurement, Laser instrument

Introduction

The understanding of physics of water jet discharging into the air is very important for engineering applications, such as fire-fighting equipment, cutting machines and impulse turbines. For this importance, many researchers have worked intensively on the study of water jets.

Hoyt et al. studied water jets discharging into the air with using special photography techniques [1-4]. In their studies, they focused attention on laminar-turbulent transition and droplet formation. They also examined the jets of water solution of polymer and found that the polymer reduced small-scale disturbances on the jet surface.

Yanaida researched the characteristics of high-speed water jets discharging into the air [5]. He determined the width of jet spreading with using the electric measuring method. It was found that the jet spreading width does not depend on pressure and type of fluid, and that the width is proportional to the square root of the distance from nozzle exit. The proportional constant is affected by nozzle shape.

Brekke examined the velocity distribution in a water jet for the application to Pelton turbine [6]. The nozzle with 2 or 6 fins was connected to a bend pipe. A miniature Pitot tube was arranged just downstream of the nozzle. The effect of fin and bend on velocity was indicated.

In order to design a Pelton turbine, Zhang et al. developed a laser Doppler anemometry (LDA) method and investigated water jets discharging into the air with using the LDA method [7, 8]. They used two types of the pipe connected to a nozzle. One was a straight pipe, while the other was a 90-degree bend pipe. They measured the velocity distribution in the jet with the LDA method and discussed the effect of bend on velocity distribution. They obtained the result that the bend strongly affects the flow in the jet.

Various contact measuring methods were employed to obtain flow characteristics, such as jet spreading width and velocity distribution, in these previous works. In the velocity measurement with a Pitot tube, the tube penetrated the water jet. In the electric measuring method, electric probes touched the water jet surface. In the LDA method, an optical wedge contacted the jet surface in order to ensure that laser beams transmit through the jet surface. The contact with a water jet surface would affect flow characteristics undesirably.

There are many important characteristics of water jets, but we focus attention on jet spreading width in this paper. We employ the non-contact measuring techniques with a laser instrument in order to avoid an undesirable effect of the contact with a water jet surface.

The motion of a water jet surface is unstable and unsteady as one can see Hoyt's photographs [1-4] for example. We consider this unstable motion and assume that a water jet can be divided into three regions: core region, intermittent region and spray region. Our measuring techniques take into account this water jet structure.

The objective in this paper is to examine the feasibility of our measuring techniques and to obtain the data of jet spreading width for future applications.

Water jet structure

The shape of water jet surface changes unsteadily because of turbulence, hydrodynamic instabilities and so on. For examples, Hoyt et al. observed instability waves on the surface, air entrainment and droplet generation from the surface [1-4].

A water jet in our experiment is shown in Fig. 1. As one can see in Fig. 1, the water jet surface moves unsteadily. The surface shape is wavy and a lot of droplets arise from the surface. Considering these unsteady motions of the surface, we assume the jet structure as shown in Fig. 2.

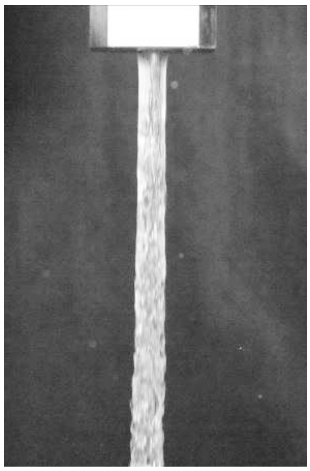

Fig. 1 Water jet in our experiment (Total head is 21 m. Needle stroke is 9 mm.)

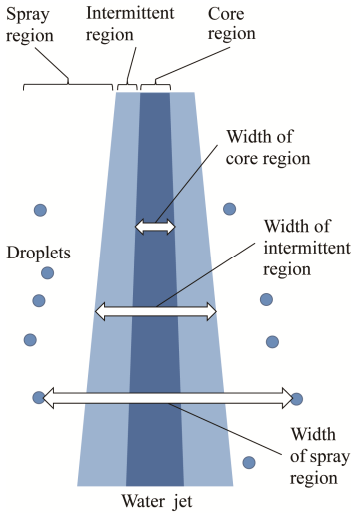

Fig. 2 Water jet structure

The *core region* is defined as the stable standing region in the jet, while the *intermittent region* is defined as one where the unsteady wavy jet surface passes. The region where the droplets exist is called the *spray region*. The width of each region is measured in the experiments.

Experiments

Apparatus

Figure 3 shows the schematic of the experimental apparatus which is the same one used for stationary Pelton bucket experiments [9]. The maximum head of the water in this apparatus is 28.5 meters. The flow rate is measured with an ultrasonic flow meter. The pressure is measured with a pressure transducer. These measuring instruments are located upstream of the nozzle. The jet spreading width is determined with a laser dimension measuring instrument. The detail of the width measuring method will be described later. Pictures of the water jet are taken from the front of the jet by using a digital camera and a lighting equipment.

There is a needle in the nozzle in order to adjust the flow rate. The nozzle internal structure is shown in Fig. 4. The needle is supported by ribs in the nozzle. This type of nozzle with a needle often is used in an impulse turbine. Needle stroke, S_n, is defined as the stroke from the location of the needle when the nozzle is completely closed. The jet spreading widths are measured from the direction normal to the surface made by the ribs. In other words, this direction means the laser beam direction.

Jet spreading width measurement

Jet spreading width is one of the important characteristics of water jet. The width is measured with the non-contact measuring technique, i.e. laser dimension measurement. In our experiments, the high-speed laser scan

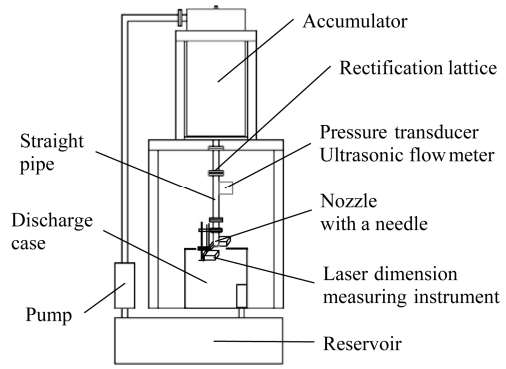

Fig. 3 Experimental apparatus

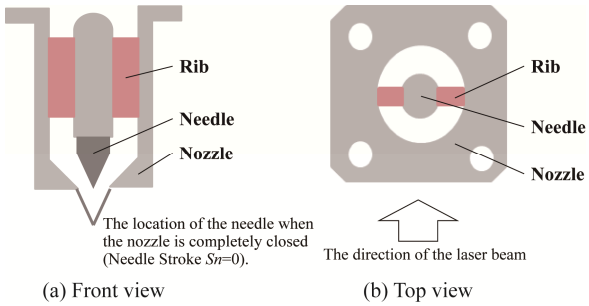

Fig. 4 Nozzle internal structure

micrometer, LS-5040, made by the KEYENCE corporation is used. The specifications of this micrometer are shown in Table 1. This micrometer is composed of a transmitter and a receiver. The transmitter emits sheet-like laser beam and the receiver receives the beam. A water jet is located between the transmitter and the receiver as shown in Fig. 5. The water jet interrupts the beam from the transmitter and makes a shadow on the receiver. The width of this shadow is measured, which is called "DIA mode."

A water jet surface is wavy and a water jet generates droplets from the jet surface. The measured value of the shadow width may vary from instant to instant, owing to the wavy surface and the droplets interrupting the laser beam. Hence two modes of measurement are employed. One is "bottom-hold mode." The minimum width of the shadow in the intended duration is recorded in the bottom-hold mode. It can be considered that this minimum value correlates with the width of core region at a given axial position of the jet. The other mode is "peak-hold mode." The maximum width in the intended duration is recorded in the peak-hold mode. This maximum value is greatly affected by the droplets and means the width of spray region at a given axial position of the jet. In our experiments, these two modes are used at a time, and both minimum and maximum values are recorded. The recording duration of both modes is set to 10 s. The accuracy of the laser scan instrument is confirmed by measuring the width of an accurately finished 30-mm diameter calibration cylinder before and after experiment.

Table 1 Specifications of the laser scan micrometer, LS-5400, KEYENCE

Laser scan rate	1200 scans/s
Laser scan velocity	121 m/s
Laser scan range	Approx. 46 mm

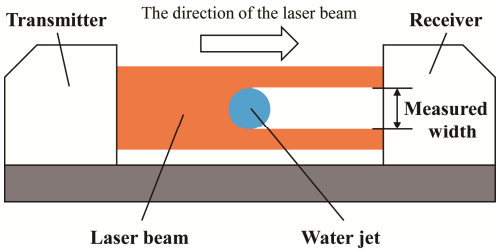

Fig. 5 Configuration of the laser scan micrometer

Pictures of a water jet are taken with a scale in a room surrounded in blackout curtains. Only the transmitter of the laser scan micrometer is used during photography. A water jet is set up between the transmitter and the scale. The laser beam is emitted to the scale. The width of the water jet shadow on the scale is measured from the pictures as shown in Fig. 6. In photography, the digital single-lens reflex camera, D7200, made by the Nikon corporation is used. The lens is AF-S DX NIKKOR 16-80mm f/2.8-4E ED VR made by Nikon. This special lens has Nano Crystal Coat for reducing the ghost and flare phenomena. The settings of the camera are shown in Table 2. If the exposure time is shorter than the laser scan time (i.e. the inverse of the laser scan rate), the laser beam on the scale cannot appear in the picture. Hence the exposure time must be set to sufficiently longer value than the laser scan time. This means that the picture of the laser beam taken by the camera is the integrated image over the longer time than the laser scan time. It can be considered that the shadow width in the picture as averaged interruption width of the laser beam by the jet is close to the width of intermittent region.

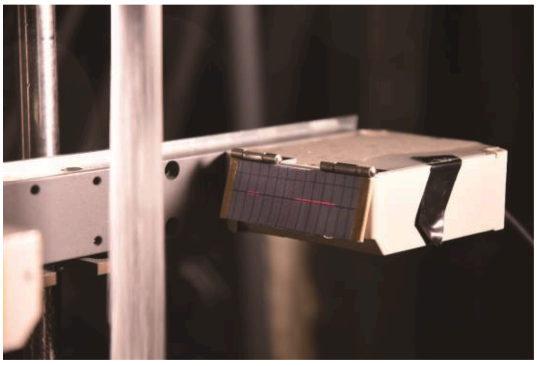

Fig. 6 Picture of the water jet and the scale for measuring the shadow width

Table 2 Settings of the camera

Aperture	4.0
Exposure time	1/250 s
ISO	800
Focal length	80 mm

The x coordinate is set to the jet axis and its positive direction corresponds to the flow direction. The origin of the x coordinate is located at the position of the needle tip. The range of measurement is from x = 0 [mm] to x = 100 [mm]. The interval of the measuring points is 2 mm between x = 0 [mm] and x = 20 [mm], 10 mm between x = 20 [mm] and x =100 [mm]. In an experiment, the number of measurements with the laser scan micrometer on both the bottom-hold and peak-hold mode is 25 at each measuring point. The number of photographing is 20 at each measuring point.

Experimental conditions

In all experiments, the total head of the water jet, H, is set to 21 m. Three needles different in length are employed and these needle strokes are 14, 9 and 4 mm. The relation between needle stroke, S_n, and flow rate, Q, is shown in Fig. 7.

Results

Scatters of the jet spreading widths measured in a typical experiment

The results in a typical experiment are shown in Fig. 8. In this experiment, the needle stroke is set to 14 mm. The symbols in Fig. 8 mean the measured values of jet spreading widths, W, divided by the jet width or diameter at the nozzle exit, W_0. This width, W_0, is calculated with Bernoulli's principle and the equation of continuity. While there are 25 symbols for the jet spreading width of both the core and spray region at each measuring point, 20 symbols exist for the jet spreading width of the intermittent region. The number of each symbol equals to that of each measurement described above. The lines in Fig. 8 are made by connecting with lines the averaged values at each measuring point.

In the widths of all regions, the scatter of the measured data is small upstream but relatively large downstream. The data of the width of the spray region have the largest scatter in the three regions, while the scatter of the width of the core region is the smallest. These tendencies are consistent with the visual observations, and correlate to unstable and unsteady characteristics of a water jet.

Averaged values of jet spreading widths

Three experiments were performed in each setting of needle stroke, S_n. The experimental results in the case of S_n = 14 [mm] are shown in Fig. 9. The symbols in Fig. 9 mean the averaged values of jet spreading widths in each experiment as explained in the previous section. The jet spreading widths, W, are non-dimensionalized by dividing by the jet width at the nozzle exit, W_0.

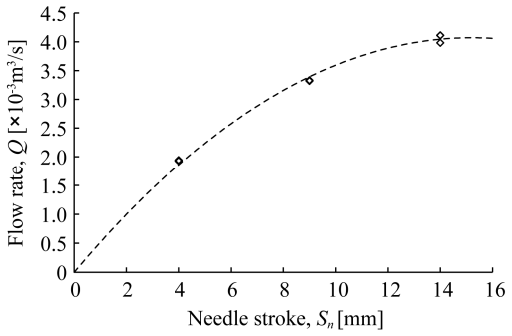

Fig. 7 Relation between needle stroke and flow rate. The points are the measured values in the experiments. The dashed curve is obtained by fitting the origin and the experimental data to a quadratic curve with the least-square method.

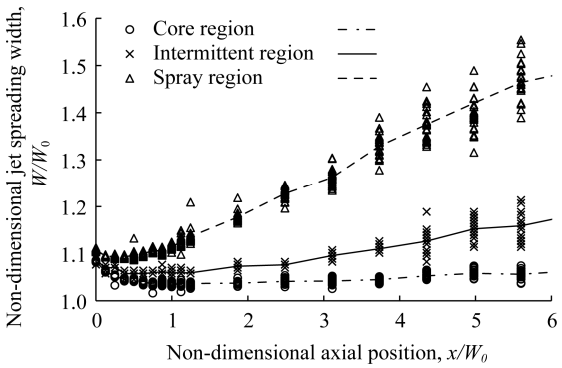

Fig. 8 Jet spreading widths in a typical experiment (H = 21 [m], S_n = 14 [mm]). The symbols are the measured values. The lines connect to the averaged values at each measuring point.

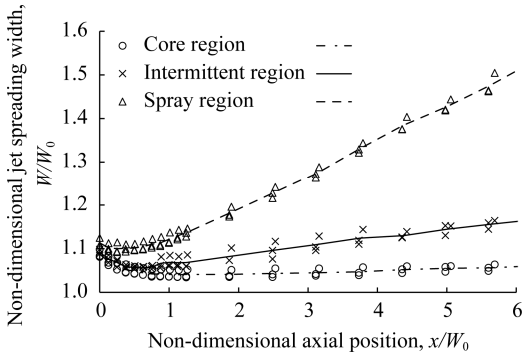

Fig. 9 Jet spreading widths in the case of S_n = 14 mm. The symbols are the averaged values in each experiment. The lines connect to the averaged values of three symbols at each measuring point.

Table 3 Averaged jet width at the nozzle exit

Needle Stroke, S_n [mm]	Averaged jet width at the nozzle exit, W_0 [mm]
14	16.0
9	14.5
4	11.0

The averaged W_0 values obtained from the W_0 values in each experiment are listed in Table 3. The lines in Fig.9 are made by connecting the values obtained by averaging the values of the symbols at each measuring point.

As one can see in Fig.9, the magnitude relation between the widths of the three regions is consistent with the initially assumed jet structure in Fig. 2. The width of the spray region is larger than that of the intermittent region. The intermittent region has larger width than the core region.

The non-dimensional jet spreading widths, W/W_0, of the three regions decrease with increasing the non-dimensional axial position, x/W_0, near the nozzle exit. After passing over the inflection point, the widths, W/W_0, increase. While the width of the spray region has the highest increasing rate, the width of the core region has the lowest rate.

The experimental results in the case of S_n = 9 [mm] and S_n = 4 [mm] are shown in Fig. 10 and Fig. 11, respectively. These results have almost the same tendencies as that of the case of S_n = 14 [mm]. However, in the case of S_n = 4 [mm], the width of the core region decreases almost monotonously with increasing x/W_0. The cause may be that the flow rate in the case of S_n = 4 [mm] is very low as shown in Fig. 7.

The widths of the three regions decrease with decreasing the needle stroke, i.e. decreasing the flow rate, as shown in Figs. 9-11.

Effect of needle stroke on jet taper

Another important characteristic of water jets is jet taper or increment ratio of jet width in the jet direction. Especially, the engineers in the field of impulse turbine take account of this characteristic. For example, Oyamada et al. examined the effects of the nozzle and needle geometry on jet taper [10].

In almost all results of our experiments, there are the inflection points of the widths between x/W_0 = 0 and x/W_0 = 2. Hence jet tapers are calculated with the data of the widths between x/W_0 = 2 and x/W_0 = 6, after passing over the inflection points. In this range of x/W_0, all data of the width of each region are fitted to a line with the least square method. The slope of the line, $\Delta W/\Delta x$, is a jet taper.

The jet tapers in our experiments are shown in Fig. 12. Except for the intermittent region, the jet tapers increase with increasing the needle stroke. The value of jet taper in S_n = 9 [mm] is the largest in the intermittent region. Only the jet taper of the core region in S_n = 4 [mm] has a negative value.

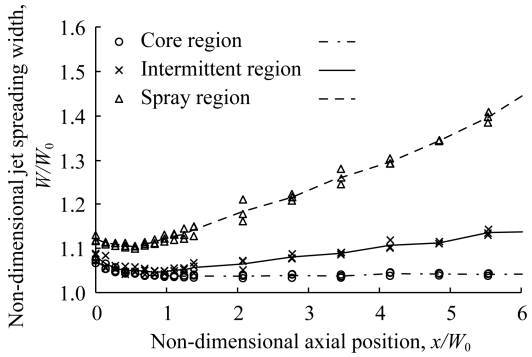

Fig. 10 Jet spreading widths in the case of S_n = 9 [mm]. The symbols are the averaged values in each experiment. The lines connect to the averaged values of three symbols at each measuring point.

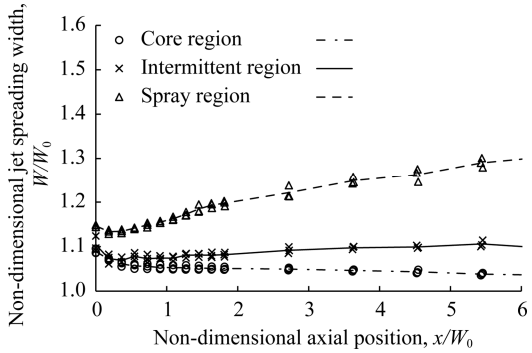

Fig. 11 Jet spreading widths in the case of S_n = 4 [mm]. The symbols are the averaged values in each experiment. The lines connect to the averaged values of three symbols at each measuring point.

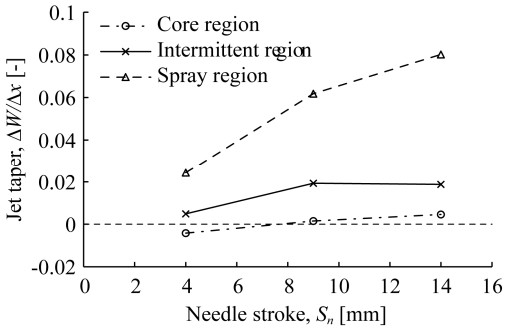

Fig. 12 Jet taper

Conclusions

The non-contact measuring methods with a laser instrument were introduced in order to obtain the data of jet spreading width which is one of the important character-

ristics of water jets. The experiments on various needle strokes were performed with the measuring methods. These results were consistent with the water jet structure. Hence it can be concluded that our non-contact measuring methods are feasible for getting the jet spreading widths.

The data of jet spreading widths and jet taper were obtained on various needle strokes. These data are useful for future applications, such as the design of impulse turbines.

While there are lots of works including our research, physics of water jet discharging into the air is yet inadequately understood. Especially, there is not adequate knowledge about the effects of nozzle conditions, such as nozzle shape, nozzle internal structure and inlet bend, on the flow in water jets. Studying these effects with our measuring methods is a future work.

Acknowledgements

The authors wish to thank the students, who graduated from Fluid Engineering Laboratory at Kanagawa University, for conducting the preliminary experiments.

References

[1] J. W. HOYT, J. J. TAYLOR and C. D. RUNGE: The Structure of Jets of Water and Polymer Solution in Air, J. Fluid Mech., Vol.63, Pt.4 (1974), pp.635−64.

[2] J. W. HOYT and J. J. TAYLOR: Waves on Water Jets, J. Fluid Mech., Vol.83, Pt.1 (1977), pp.119−127.

[3] J. W. HOYT and J. J. TAYLOR: Turbulence Structure in a Water Jet Discharging in Air, Phys. Fluid, Vol.20, No.10, Pt.II (1977), pp.S253−S257.

[4] J. J. TAYLOR and J. W. HOYT: Water Jet Photography – Techniques and Methods, Exp. Fluids, Vol.1 (1983), pp.113−120.

[5] K. YANAIDA: Characteristics of Water Jets, Rev. High Press. Sci. Technol., Vol.5, No.2 (1996), pp.98−102 (in Japanese).

[6] H. BREKKE: State of the Art of Small Hydro Turbines versus Large Turbines, Hydro 2005, Villach, Austria, 2005.

[7] Zh. ZHANG and E. PARKINSON: LDA Application and the Dual-Measurement-Method in Experimental Investigations of the Free Surface Jet at a Model Nozzle of a Pelton turbine, 11th International Symposium on Applications of Laser Anemometry to Fluid Mechanics, Lisbon, Portugal, 2002.

[8] Zh. ZHANG and M. CASEY: Experimental Studies of the Jet of a Pelton Turbine, Proc. IMechE, Vol.221, No.8, Pt.A: J. Power and Energy (2007), pp.1181−1192.

[9] Y. NAKANISHI, T. FUJII and S. KAWAGUCHI: Numerical and Experimental Investigations of the Flow in a Stationary Pelton Bucket, J. Fluid Sci. Technol., Vol.4, No.3 (2009), pp.490−499.

[10] S. OYAMADA, S. OKISAKI and R. SUDO: In-Site Performance Test of Pelton Turbine, OHM, Special Issue on In-Site Testing Methods for Maintenance (1957), pp.155−167 (in Japanese).